Spectroscopic SWIFT

D. Idiyatullin[1], C. Corum[1], S. Moeller[1], J. Ellermann[2], and M. Garwood[1]
[1]CMRR, University of Minnesota, Minneapolis, MN, United States, [2]Radiology, University of Minnesota, Minneapolis, MN, United States

INTRODUCTION Often the ability to obtain chemical-shift information is needed and advantageous in MRI. In addition to providing chemical information, the acquired spectral dimension can also be used to reduce image blur resulting from frequency shifts of all types. This work describes a new 3D and 4D spectroscopic technique involving an intrinsic frequency dimension. The method is based on an old idea to reveal both the spatial distributions and intrinsic frequency spectra of NMR signals from a set of projections obtained in the presence of fixed spatial gradients of varied strength and orientation [1]. Instead of collecting the FID after applying a hard RF pulse, as done in the original method, the new technique uses SWIFT (SWeep Imaging with Fourier Transform) [2], which is less demanding of RF field amplitude, and therefore, is more applicable to human study [3]. Due to the absence of an "echo time" in the SWIFT sequence, the presented method can be applied for spectroscopy of objects having transverse relaxation times, T_2, in microsecond time scale. Consequently the main application of this method is expected to be in ultra- short T_2 mapping, which is in the focus of this work. Other applications such as fat-water separation and imaging near metallic implants will be illustrated and discussed.

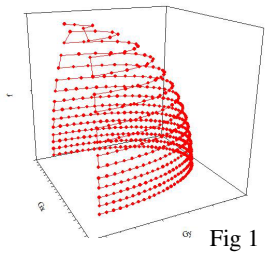
Fig 1

THE DESCRIPTION OF THE METHOD In the presence of a field gradient of strength G the angle, θ, between the direction of a projection and the frequency axis in the "pseudo space" is given by $\theta \approx \mathrm{atan}\left(\gamma GD/\Omega\right)$ for an object confined to a range D in the spatial dimension and Ω in the frequency dimension [1]. The amplitude of the gradient is varied to obtain a set of directions, θ, distributed in the 2 or 3 spatial and one spectroscopic "pseudo space". Since θ is incremented by changing the gradient strength, the bandwidth of each projection increases with increasing θ angle. To compensate for this, the projections are scaled by setting the acquisition bandwidth as $b_w = \Omega/\cos\theta$. For isotropic image resolution the orientation of the "pseudo vector", which is a sum of vectors G and Ω, must be uniformly distributed in the "pseudo space". In case of isotropic 3D (2D spatial and one spectroscopic dimension) the terminal of this vector must describe a hemisphere. The case was implemented as N_f circles equally spaced every $\Delta\theta$ and increasing radius with θ angle hence the number of points (each presenting one projection) on circles is changing as $2\pi sin(\theta)/\Delta\theta$. Correspondingly, in the 4D case, there are N_f growing spheres, each having $4\pi sin(\theta)/\Delta\theta^2$ number of uniformly distributed points. To uniformly cover the spheres we used a slightly modified generalized spiral points trajectory [4]. In practice 4D isotropic imaging is very time consuming. However, in most applications the resolution in the spectroscopic dimension can be much less than in the spatial dimensions. Decreasing the sampling density in the spectroscopic dimension was reached by increasing $\Delta\theta$ with decreasing θ angle. Angles for such experiment were calculated as $arctan[P\cdot tan(\theta)]$, where P is the scaling parameter for the sampling in spectral dimension. $P = 1$ for fully isotropic case and $P > 1$ for decreased sampling density in the spectral dimension. **Figure 1** shows half set of spokes for a 3D experiment with $P = 2$. Another half is acquired with the gradient directions inverted. **Figure 2** presents the gradient and bandwidth changes during a 4D experiment with $P = 2$. The figure describes 6 shrinking hemispheres in time. The opposite hemispheres are also acquired using inverted gradient directions. The applied order of projections can be changed to avoid high gradient steps and/or achieve a desirable steady state condition for a magnetization. Depending on the application the scaling parameter P was varied from 1 till 16. The effect of different P on a broadening of spectroscopic and spatial point spread functions based on the simulated and experimental data will be presented and discussed. For the reconstructed of 3D and 4D dataset the gridding method [5] was used.

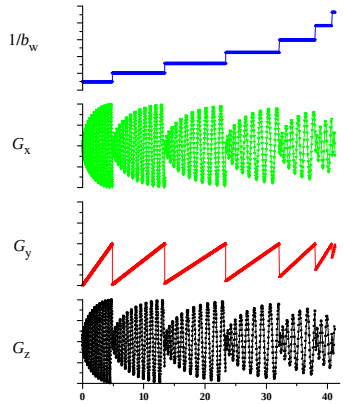

Fig.2

EXPERIMENT AND DISCUSSION A 4mm axial slice of a lamb bone in the tibiofibular joint vicinity was used for *in-vitro* imaging with a 1cm loop surface coil on a 4.7T Varian INOVA scanner. The total number of projections was 5246, with 256 complex points acquired during each projection, $P = 2$, diameter of $FOV = 3$ cm, $b_{w,max} = 62$ kHz, $\Omega = 6$kHz, flip angle 11°, and total acquisition time 20 min. **Figure 3 a-e** are MIP's of the 3D spatial-spectroscopic SWIFT images over different spectral subsets. In **Figure 3a** a MIP of all spectral slices is shown. The rest are MIP images over selected chemical shift ranges, which are: (b) (-2 ppm, 0 ppm), (c) (0 ppm, 2.5 ppm), (d) (2.5 ppm, 5 ppm), (e) (5 ppm, 7.5 ppm). The

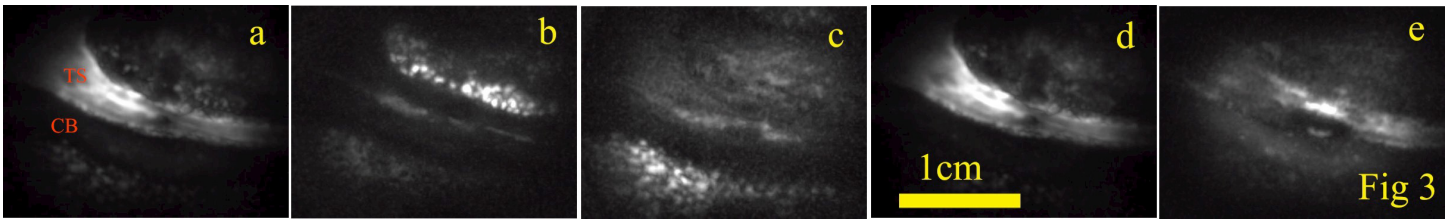

images are scaled differently to set optimal brightness. The tibiofibular syndesmosis (TS) has a brightest signal in non-selective MIP (**a**) and in image (**d**) with spectral band close to water resonance. A trabecula bone enclosing islands of fatty bone marrow is visible in images (**b**) and (**c**). The spectral linewidth of cortical bone (CB) is comparable with spectral window Ω and should have contribution in all images. However, signal from CB is shadowed by high signal from fatty tissue or TS. Only in image (**e**), which contains frequencies higher then water and fat resonances, the CB of tibia is slightly visible. A T_2 map can be obtained by coloring the spatial images based on the average T_2 of corresponding spectra.

ACKNOWLEDGMENTS This research was supported by NIH P41 RR008079 and the Keck Foundation.
REFERENCES **[1]** M. L.Bernardo,et al., J.Magn Reson. (1985). **[2]** D.Idiyatullin, et al. J.Magn.Reson.(2006). **[3]** D.Idiyatullin, et al. J.Magn. Reson. (2008) **[4]** E. B. Saff, et al. Mathematical Intelligencer (1997) **[5]** J. I. Jackson, et al., IEEE Trans. Med. Imaging (1991).